# 4. FREE SURFACE GROWTH AND DISSOLUTION UNDER FLOW

As fluids flow more quickly, advective transport begins to dominate over diffusive transport and a transition from diffusion limited precipitation and dissolution to an advection dominated regime occurs. This transition is often quantified by the dimensionless *Peclet* number, which is a measure of the relative importance of advective and diffusive transport over a characteristic distance such as the overall size of the system or the typical size of a feature of interest. It is the ratio between the fluid velocity and the diffusion coefficient, multiplied by the characteristic length. Peclet numbers much larger than unity imply advection dominated transport. Reactive transport under moderate to high velocity, large conduit or open channel flow can give rise to extremely rich and complex patterns in *e.g.* hydrothermal, karst and travertine systems, in glacial and volcanic settings, and in any systems involving weathering, erosion and deposition by the agents of water or wind. Indeed, reactive, advective, open flow is at least partly responsible for most of the abiotic geometry seen on the surface of the Earth. Again, these systems can be classified in a sequence of increasing complexity.

## 4.1 Steady, unidirectional flow, ballistic models

The simplest possible flow model is that of unidirectional advection with constant velocity. Such a model is of course unrealistic because it does not include the modification of flow by obstructing objects but it can be a useful abstraction. The ballistic deposition model is a discrete particle model of growth under unidirectional flow (Meakin, 1998).

The dominating feature of these models is that growth occurs predominantly in the direction against the flow, where the concentration gradients are steepest. The introduction of a directional external field breaks the perfect, spherical symmetry of simple or diffusion controlled, surface normal growth (Fig. 4.1a). These patterns are in many respects similar to step patterns in natural travertines or geyserites, as can be observed around hot springs (Fig. 4.1b) but these grow away from the fluid source rather than toward the flow.

## 4.2 Stokes, laminar and shallow water flow

The most general equations for fluid flow are the Navier-Stokes equations for compressible fluids. This set of equations can, in principle, be used to model flow of any complexity. However, for many geological problems, it is not necessary to include the full set of terms. For water, we can assume that the fluid is incompressible and for the case of very low velocities, high viscosities, or flow in very small systems, such as small pore or crack networks in rocks, we can furthermore assume that the inertial forces are small compared with viscous forces. Under these circumstances, the incompressible Stokes equations:

$$\nabla p = \mu \nabla^2 \mathbf{v} + \mathbf{f}$$
$$\nabla \bullet \mathbf{v} = 0 \qquad (4.1)$$

can be used instead of the nonlinear Navier-Stokes equations. Here, $p$ represents the pressure (scalar), $\mathbf{v}$, the velocity (vector field), $\mu$, the dynamic viscosity and $\mathbf{f}$, the applied force per unit volume. The first equation describes the relationship between the pressure gradient and the viscous forces, while the second (zero divergence) ensures that the rate of transport into a control volume is equal to the rate of transport out of it so that mass is conserved.

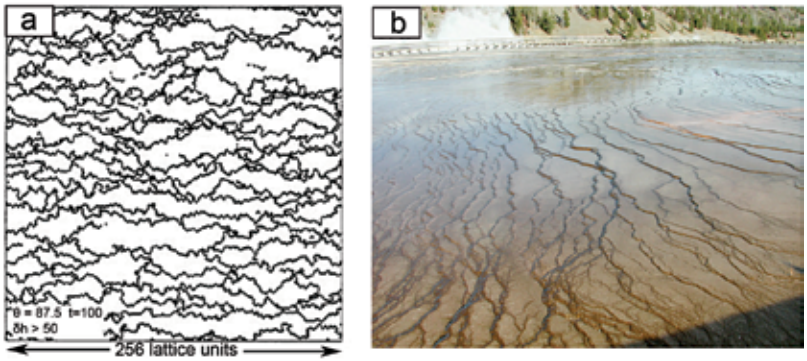


**Figure 4.1** a) Top view of a three dimensional simulation of ballistic deposition onto an initially flat surface with an oblique angle of incidence, producing anastomosing step edges (from Meakin and Krug, 1990, with permission from the European Physical Society). b) Geyserite steps around Grand Prismatic spring, Yellowstone National Park. Geyserite is a form of opaline silica often found around hot springs and geysers. The fence and trees in the background provide scale.

*Water is the driver of nature.*

LEONARDO DA VINCI (1452-1519), *Thoughts on Art and Life*

For faster flow or in larger flow domains, the Stokes equations become inaccurate. It is then necessary to reintroduce the terms for conservation of momentum included in the Navier-Stokes equations. If thermal gradients are important, an energy conservation equation is also needed. For relatively low

velocities, flow is laminar or nearly so, meaning that there is limited flow separation and eddies are large and simple. Under such conditions, the numerical methods for approximating the solution to the Navier-Stokes equations are relatively simple and accurate. However, accurate simulation of highly turbulent (high Reynolds number) flow is still very challenging.

Photo: Dag K. Dysthe, PGP.

**Figure 4.2** Travertine terraces at Mammoth hot springs, Yellowstone National Park, Wyoming, USA. The fenced footpath near the upper left corner provides scale.

## 4.3 Travertine terraces

Travertine terraces (rimstone) are spectacular, often intricate structures formed when calcium carbonate (calcite and also often aragonite) precipitates under running water (Fig. 4.2). Travertine terraces and other deposition patterns form over a wide range of scales from millimetres to tens of metres, in diverse settings, such as hydrothermal springs, cold mountain streams and limestone caves.

Travertine terracing is an excellent example of a complex system that develops self organised patterns with numerous positive and negative feedback paths. The emergence of patterns in such systems is not trivial and intuition often fails us. Our group and the group of Nigel Goldenfeld at the University of Illinois at Urbana-Champaign have studied travertine terracing in detail using a fruitful combination of field observation, laboratory experiments and computer modelling (Jettestuen *et al.*, 2006; Goldenfeld *et al.*, 2006; Veysey and Goldenfeld 2008; Hammer *et al.*, 2007; 2008; 2010). A particularly interesting aspect of this work was the way in which we attacked the problem at many different levels of abstraction, in order to answer several types of questions.

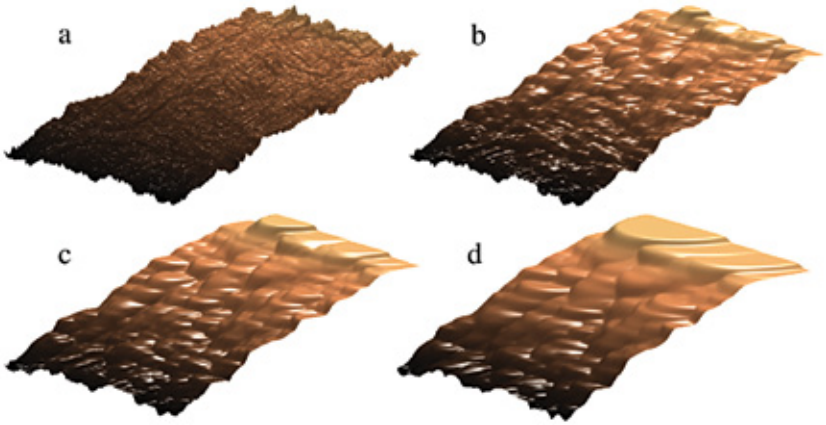


**Figure 4.3** Four stages in the development of terraces from the simulations of Jettestuen *et al.* (2006). Terrace patterns emerge when growth is proportional to the local slope (from Jettestuen *et al.*, 2006, with permission from Elsevier).

From a purely geometric perspective, terrace patterns can be produced by a surface normal growth model based on the assumption that the growth rate is proportional to the local slope (Fig. 4.3; Jettestuen *et al.*, 2006). Clearly, there can be no pattern formation if the initial slope is perfectly flat and smooth because the growth rate is then constant across the surface. In such simulations we therefore usually start with a slightly rough surface. Variations in the surface height grow in response to positive feedbacks, while negative feedbacks regulate the system. In this case, any small protuberance increases in the downstream direction, where the slope is high, while flat tops stop growing and remain level.

So far the model is geometric and abstract, and it remains to connect it to mechanisms operating in nature. The morphology emerging in these simulations resembles the small scallops that form on near vertical, travertine walls covered by a thin layer of flowing water. The flow velocity is, to a first approximation, proportional to slope. These results therefore indicate a relationship between flow velocity and precipitation rate. This relationship has indeed been observed and quantified in field studies by many authors. The simulation can be made more realistic by modelling the fluid flow over the surface using the Navier-Stokes equations and specifying a linear relationship between local flow rate and the surface-normal growth rate (we have not yet explored the mechanism for this relationship). A simplification of the Navier-Stokes equations is provided by using the shallow water approximation, where flow is averaged over depth. We found that this results in a morphology that is more reminiscent of larger terraces on less steep slopes (Hammer *et al.*, 2007). The model reproduces several peculiarities of travertine terrace growth observed in nature, such as downslope migration of steps, coarsening by merging and drowning of upstream steps and stretching of

dams in the downslope direction. Goldenfeld *et al.* (2006) and Veysey and Goldenfeld (2008) developed a somewhat similar model, with further simplification of the flow (using a discrete model for Stokes flow) but including several other processes such as surface tension and simplified chemistry and heat transport. These simulations also assumed a relationship between flow velocity and precipitation rate, producing very realistic terrace patterns.

Our simulations (Hammer *et al.*, 2007) demonstrated that a simple flow/precipitation relation is sufficient to explain terracing and its dynamics. This is certainly not a trivial result and could not have been easily achieved by observation or laboratory experiments alone because it is not possible to reduce the real system to such bare essentials. A large number of confounding effects, including biological processes, make it almost impossible to isolate the interactions responsible for the pattern formation. However, the model was still not mechanistic, in the sense that the flow/precipitation rate relationship was simply imposed, without fully understanding the cause of this relationship. This lack of attention to detail, which might seem unconventional, was intentional, as discussed in Section 1.2.2.

The overall reaction for the precipitation of $CaCO_3$ under normal (not hyperalkaline) conditions can be written in a highly simplified manner as:

$$Ca^{2+} + 2HCO_3^- \Leftrightarrow CO_2 + CaCO_3 + H_2O. \quad (4.2)$$

By this reaction, carbonate precipitation produces $CO_2$, which can be removed from solution by degassing. This might seem counter intuitive but calcium bicarbonate is much more soluble than calcium carbonate and $CO_2$ degassing can drive the conversion of bicarbonate to carbonate. This observation was the basis for traditional ideas about travertine terracing, involving enhanced degassing at terrace edges. At edges, water is shallower, giving a higher surface to volume ratio and therefore faster degassing. The shallow depth also requires higher flow velocity to maintain the flux, possibly explaining the velocity/precipitation rate correlation. In addition, degassing is enhanced by strong agitation at step edges. Enhanced degassing caused by pressure drop, following Bernoulli's principle (Venturi effect), has also been suggested but is unlikely, considering the small velocity gradients in this system.

In order to identify the dominating mechanism, we developed a detailed model with as little abstraction as possible (Hammer *et al.*, 2008). The model simulated free surface fluid flow over a small obstruction, in a 2D vertical section, using the full Navier-Stokes equations without turbulence modelling. The solution chemistry was modelled, with all relevant reaction kinetics involving $CO_2$, carbonate, bicarbonate, calcium and pH. All species were transported by advection and diffusion. Carbonate precipitation and degassing were derived from local concentrations. The model was successfully validated by comparison with a laboratory experiment using the same geometry and water composition, in

which the precipitation rate was mapped using an optical technique. As expected, the precipitation rate was higher in regions of faster flow over the obstruction (Fig. 4.4).

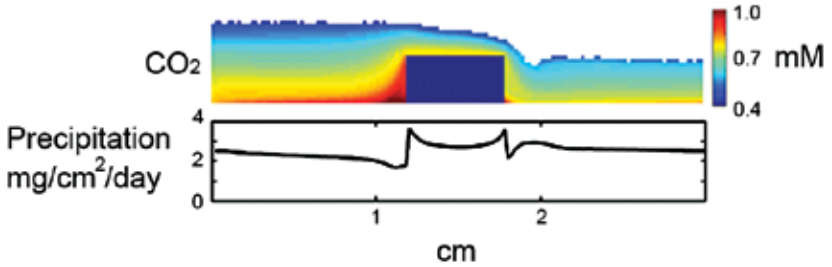


**Figure 4.4** 2D simulation of free surface water flow (left to right) over a rectangular obstruction, coupled with aqueous carbonate chemistry, degassing and calcite precipitation on the solid-water interface. Colours show $CO_2$ concentrations in mM (from Hammer *et al.*, 2008, with permission from Elsevier).

The purpose of this detailed modelling was twofold. First it confirmed that we had understood and included the basic processes responsible for the spatial distribution of precipitation rates. Second, the model provided an experimental system which we could use to study the effects of these processes in isolation. Most importantly, we were able to switch off the variation in degassing completely, without noticeable effects on the distribution of precipitation. This demonstrated that while degassing is necessary to drive the precipitation on larger scales, local variation in degassing by hydrodynamics does not contribute to pattern formation, at least for small scale travertine terracing. The reason is that complex advection and mixing prevents degassing patterns at the air-water interface from reaching the water-solid interface where precipitation occurs.

We now believe that instead of degassing, the mechanism responsible for the velocity/precipitation correlation in this particular system is concentration gradients through the water column that are compressed when water is forced through a region of shallower water. This provides an immediate, local effect at the water-solid interface, accelerating precipitation there. Even this quite detailed model relies on empirical relationships that are not explained by fundamental principles. In particular, the rate law for precipitation is still insufficiently known and remains an important source of uncertainty. In principle, even more detailed simulations could be used to address the microscopic details of carbonate precipitation, *e.g.* using molecular dynamics. However, because of computational complexity, such a simulation would have to focus on a tiny region of the solid-fluid interface and could not answer questions about the larger scale emergent properties such as our simulations were able to do.

## 4.4 Stalactites

For the laminar, thin film water flow on the surface of a stalactite, it is possible to give analytical equations for the film thickness, $h$, and the water velocity, $u_0$, at the water-air interface. Using the Stokes flow formulation, and inserting relevant physical constants (viscosity and acceleration of gravity), Short *et al.* (2005) derived the simple equations:

$$h \approx 11\mu\text{m}\left(\frac{Q}{R\sin\theta}\right)^{1/3} \text{ and} \tag{4.3}$$

$$u_0 = 0.060\,\text{cm/s}\left(\frac{Q^2\sin\theta}{R^2}\right)^{1/3}, \tag{4.4}$$

where $Q$ represents the volumetric flux of water in cm$^3$/h, $R$, denotes the radius of the stalactite in cm and $\theta$, the angle of the stalactite surface with respect to the horizontal. Under usual conditions for stalactite formation, the film thickness is on the order of a few tens of micrometres and the velocity is less than a few mm/s. The flow velocity deeper in the film is assumed to follow a parabolic profile toward zero velocity at the solid-liquid interface (no slip boundary). Coupling these relationships to the carbonate precipitation system, it is possible to deduce an analytical expression for the growth velocity normal to the surface. Over time, this leads asymptotically to a stalactite shape described using rescaled values, $z'$ and $r'$, that represent the vertical coordinate, $z$, and the local radius, $r$, (see Short *et al.*, 2005, for additional details):

$$z'(r') \approx \frac{3}{4}(r')^{4/3} - (r')^{2/3} - \frac{1}{3}\ln r' + \text{constant}. \tag{4.5}$$

This analysis does not include effects that could lead to the smaller scale instabilities with a characteristic wavelength (ripples or rings) that are commonly observed on stalactites (Fig. 4.5). These instabilities presumably originate from a process in which local protrusions induce their own growth, *e.g.* by enhanced degassing, but short wavelength features are suppressed by surface energy or transport effects (*i.e.* a Mullins-Sekerka-like instability).

## 4.5 Stagnation and flow in combination

In travertine terrace systems, the water flow rate is often very slow in the deeper pools between terrace edges. In such cases, surface normal or diffusion limited growth is observed within the pools (Fig. 4.6a). In other cases, surface normal growth of "cave pearls" (Fig. 4.6b) takes place in dry or almost dry pools, where dripping water causes precipitation of carbonate minerals evenly over a surface.

Cave pearls often nucleate on a sand grain. The forces acting on cave pearls by flowing water can prevent them from sticking together and growing into botryoidal aggregates, which are also common.

Photo: George Chakonas, Northern Illinois University.

**Figure 4.5** Single stalactite with clearly visible surface ripples. Field of view: ~50 cm.

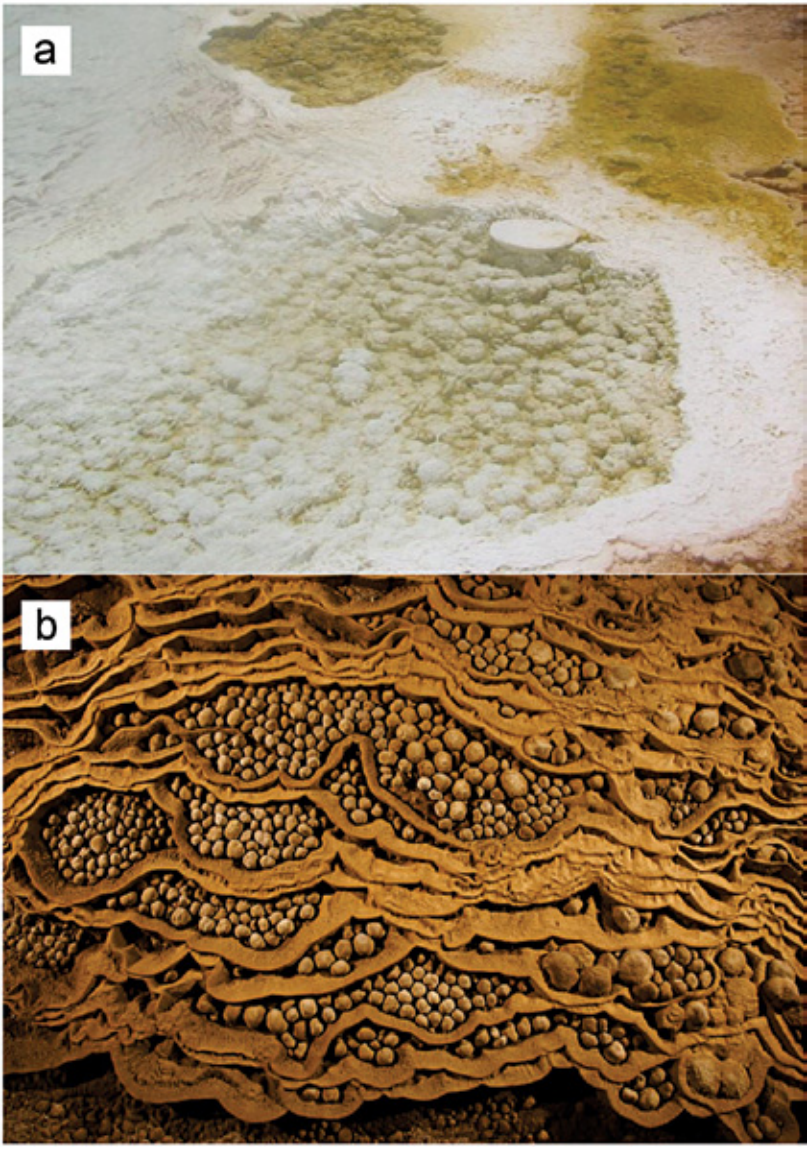


Photo: Bjørn Jamvelt.

Photo: Carsten Peter, National Geographic Magazine.

**Figure 4.6** a) Botryoidal growth of calcite in the deeper water pools of the travertine terraces at Mammoth Hot Springs, Yellowstone National Park. Field of view ~1 metre. b) Rare cave pearls (each 1-2 cm across) fill dried out terrace pools near the Garden of Edam in Hang Son Doong.

## 4.6 Biomineralisation in moving fluids

Many species of colonial corals have branching, dendritic morphologies reminiscent of those seen in DLA (diffusion limited aggregation) simulations. The branches tend to be space or plane filling but are self avoiding (Fig. 4.7). Jaap Kaandorp and his coworkers (*e.g.* 2003; 2005) have made extensive experimental, field and simulation studies on the biology and fluid dynamics of coral growth, demonstrating that the availability of nutrients (specifically inorganic carbon, Kaandorp *et al.*, 2005) in water surrounding the colony can explain the branching.

A coral colony is a self organising system, growing in response to external gradients set up by diffusion and advection but also itself modifying fluid flow and nutrient distribution that depend on its changing morphology. Applying such knowledge to fossil organisms, it might be possible to estimate environmental parameters such as the intensity and prevailing direction of currents and waves (*e.g.* Hammer, 1998).

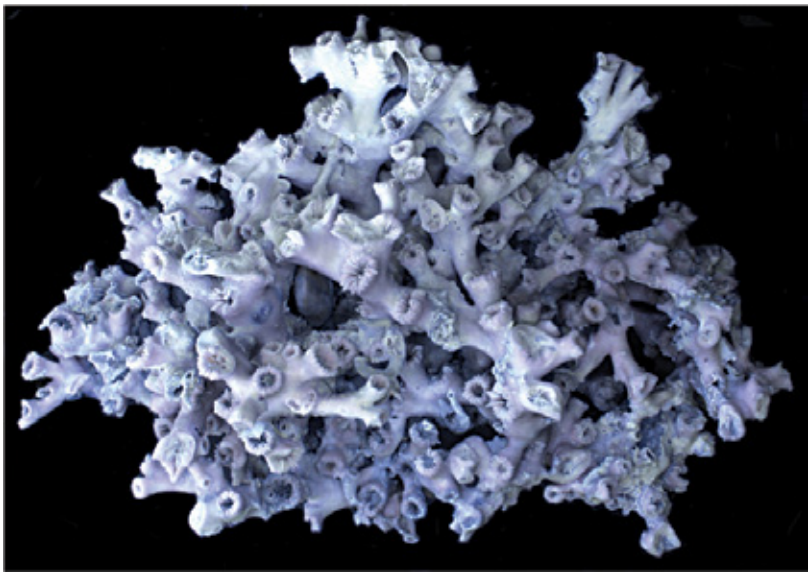

Photo: Øyvind Hammer.

**Figure 4.7** *Lophelia pertusa*, a cold water coral from the base of the Holocene, Drammenselva, Norway. Field of view ~20 cm.

## 4.7 Surface karst morphology

Some of the most beautiful landscapes on Earth result from limestone dissolution over a wide range of scales (Fig. 4.8). Karst landforms are a central theme in traditional Chinese art (Fig. 4.9), where they can appear so bizarre that Western critics often viewed them as artistic fantasies. In fact, they are usually depicted fairly realistically. Undoubtedly, these dissolution processes can be strongly influenced by pre-existing rock features, such as joints that focus fluid flow, giving rise to blocky "clints" separated by deep "grikes" (Fig. 4.8). Of special interest to us are pattern formation processes taking place in more homogeneous rocks, often at smaller scales (Fig. 4.10). The extensive karst nomenclature reflects the richness of these phenomena (*e.g.* dolines, rillenkarren, meanderkarren, rundkarren, poljes, swallets, flutes, scallops, pans, runnels, uvalas and avens).

Photo courtesy: Angus McIntyre (raingod.com).

**Figure 4.8** Karst landscape in limestones seen from the summit of Yueliang Shan, near Yangshuo.


**Figure 4.9** Tang dynasty painting of karst landscape by Dong Yuan (*ca.* 934-962 AD).

Dissolution of limestone at near neutral pH can be described in a simplified manner by the reverse reaction of Eq. (4.2). Dissolution therefore consumes $CO_2$, which can be supplied from the atmosphere. Exactly the same considerations about gas transport apply to dissolution as precipitation, just in the opposite direction. In particular, we expect a correlation between flow velocity and dissolution rate and this is what is observed. This correlation is reminiscent of the well known correlation between flow velocity and erosion rate in stream channels, usually leading to localised channelling patterns. Consequently, typical dissolution patterns in limestone produce channels in the downslope direction such as the rills (karren) observed in Figure 4.10.

Photo: Mauro Pau, PGP.

**Figure 4.10** Rillenkarren, Oliena, Sardinia, Italy, with an apparent characteristic wavelength. The area is about 2.5 m across.

Hammer (2008) suggested a simplified parameter space diagram for growth and dissolution under flow, such as that shown in Figure 4.11, in this case in the context of karst and travertines. When the flow rate is low, or growth is not strongly dependent on flow rate, botryoidal growth dominates. This is the situation in the stagnant, deeper areas of travertine pools. The upper part of the diagram represents the precipitation regime, where growth rate increases with flow rate, leading to terraced morphologies. The lower part of the diagram is the dissolution (karst) regime, where fast flow on steep slopes is typically associated with straight channel morphology (rillenkarren), while meandering channels usually arise from low flow rates on more horizontal ground.

There are clearly other parameters that contribute to controlling pattern formation in such systems. These include the effects of scale, considering that meanders also form at large absolute flow velocities if the channel cross section is large. Furthermore, this parameter space is not meant to cover sedimentary and erosive patterns in general, without modification. Although straight channels, meanders and even terraces also form in fluvial systems, other morphologies such as braided rivers, alluvial fans and levees demonstrate that additional mechanisms must be included.

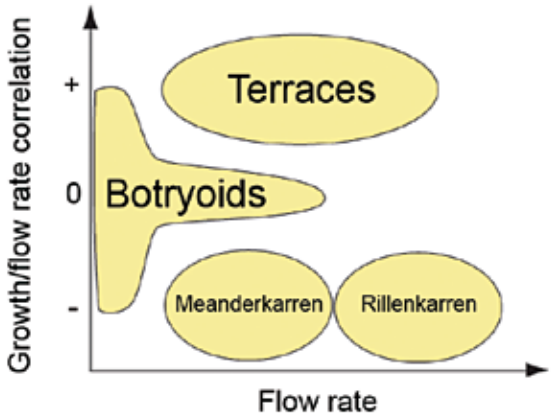


**Figure 4.11** A suggested parameter space for growth and dissolution under flow (modified from Hammer, 2008).

## 4.8 Caves and collapse

Limestone caves can form some of the largest and most spectacular dissolution structures in nature. The Cave of Swallows (Spanish: Sotano de las Golondrinas) in Mexico is a spectacular example (Fig. 4.12a). It is the largest known cave shaft in the world with a depth of about 330 m and an internal room of approximately 300 by 135 m (Fig. 4.12b). The dissolution process itself and the growth of the cavity can to some extent be modelled using geochemistry coupled with simple flow calculations. Gabrovšek and Dreybrodt (2001) simulated the emergence (speleogenesis) of networks of narrow corridors and shafts in fractured limestone in this way.

As a cavity grows, at some point the roof becomes too large to support itself, and it collapses. Such caves are often envisaged as menacing *bubbles in the Earth*, slowly ascending as the roof crumbles and the floor rises by the deposition of rubble, leaving behind a *breccia pipe*. When the bubble reaches the surface it turns into a collapse doline – an abyss that can swallow cars and houses. To model such phenomena requires coupling between dissolution and rock mechanics, typically with linear elasticity equations for deformation and some yield criterion for fracturing. Fracturing and collapse are difficult to handle with continuum modelling. Methods such as discrete element modelling (described later in this article) or discrete deformation analysis are useful.

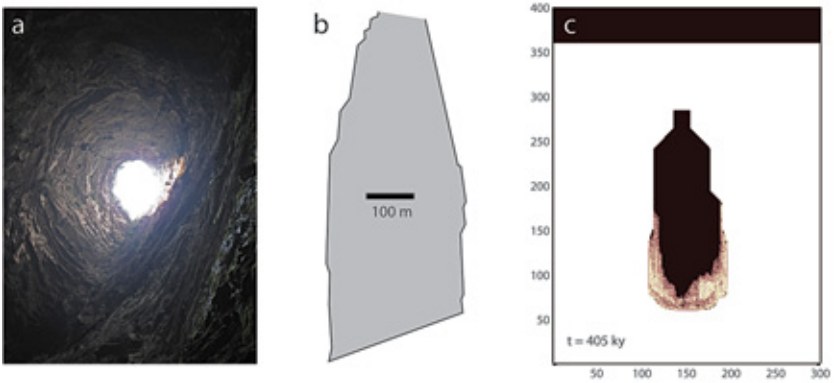


**Figure 4.12** a) Sotano de las Golondrinas, seen from within. b) Simplified profile of the Sotano de las Golondrinas collapse doline. c) Simulation of karst pipe formation. Limestone is shown in white, air or water in black and collapse material in pink. Axes are length in metres. The simulated karst pipe is shown 405,000 years after initiation (from Hammer *et al.*, in prep.).

For rock mechanical modelling it is essential to take into account structural inhomogeneities and anisotropies. Limestones are typically bedded on scales ranging from centimetres to metres. A simplifying abstraction (not fully accurate) is to consider only the strata that are not supported below and subject them to a lithostatic load from above. As a further simplification, these strata can be modelled as thin plates or, in the case of a 2D simulation, as beams. When stresses in these beams exceed a yield criterion, they break and produce rubble that falls to the floor of the cavity. Dissolution is assumed to proceed constantly, normal to the surface of both the intact walls and the collapse rubble.

Figure 4.12c shows one stage in such a simulation, just after two large collapse events that have produced upwards propagating pipes formed by an avalanche of successive collapse of overlying strata. Overhangs with straight, diagonal slopes form because this shape minimises the overhang (and therefore stress) of individual limestone benches. The overall morphology of the pipe is very similar to classical sinkholes such as the Sotano de las Golondrinas seen in Figures 4.12a and b.

*The subterranean courses of waters, like those existing between the air and the Earth, are those which unceasingly wear away and deepen the beds of their currents.*

LEONARDO DA VINCI (1452-1519), *Thoughts on Art and Life*

Such straight sloped roofs form as a result of the discrete, horizontal limestone strata forming a so called *corbel*, a *false arch* or *relieving triangle* (Fig. 4.13). In this geometry, not all tensile stresses are transformed into tangential, compressional forces. In more homogeneous rocks, other geometries are expected to form, generally with curved shapes that provide stability by directing forces downwards and outwards (*true arch*).

Photo courtesy : Clark Anderson/ Aquaimages.

**Figure 4.13** Mayan Corbel arches in Belize. A corbel vault is a construction method that uses the architectural technique of corbelling to span a space or void in a structure. The corbelled vault is a technique to support the superstructure of a building's roof.

## 4.9 Turbulent flow and boundary layers

At larger scales and flow velocities, flow becomes turbulent, unsteady and chaotic. The Reynolds number is often used to characterise the flow regime. The Reynolds number is defined as the ratio between velocity and kinematic viscosity (about $10^{-6}$ $m^2/s$ for water), multiplied by the length scale. This length scale is a matter of definition for different geometries. For flow in a pipe with circular cross section, we can use the pipe diameter as the length scale. The transition from laminar to turbulent flow happens for Reynolds numbers somewhere between 2000 and 4000, unless the wall is exceptionally smooth. This means that for water flow in pipes of less than 1 cm diameter, the flow velocity has to exceed 20 cm/s before we need to consider turbulence.

In principle, the Navier-Stokes equations are necessary to simulate turbulent flow but become extremely difficult to handle numerically because of eddies cascading down to scales too small to resolve with our computer models. In some cases, it is possible to resolve turbulent flow by direct numerical simulation using the Navier-Stokes equations. This requires very fine grids and enormous computer resources. An alternative approach is to attempt to decompose the flow field into a time averaged (steady) velocity field and additional fields that describe the turbulent motion using derived quantities such as eddy viscosity. Codes are now available for fluid dynamic simulation using a variety of different turbulence models (*e.g.* OpenFOAM and Fluent) but they are computationally intensive and typically require specification of nontrivial model parameters, numerical parameters and empirical relationships, especially at boundaries.

In many geological applications, the most important consequence of turbulent flow is that it enhances the mixing and transport of dissolved species by many orders of magnitude. Near the walls of the conduit however, turbulence is subdued because of friction and reduced velocity. This gives rise to a laminar boundary layer. Typically, the transport of dissolved species to and from a reacting surface is limited by diffusion through this boundary layer. Beyond this layer, in the turbulent core, mixing is almost total and instantaneous in comparison with the rate of purely diffusive mixing. Because the boundary layer thickness decreases with increasing overall flow velocity, this leads to progressively faster dissolution and precipitation rates under more rapid, turbulent flow (Buhmann and Dreybrodt, 1985). This provides an additional mechanism for the correlation between velocity and precipitation rate in the travertine terrace system, at least at larger scales where turbulence is important.

Photo courtesy: David Drew, Trinity College, Dublin.

**Figure 4.14** Scallops on the walls of the Polldubh Cave in the Burren, Western Ireland.

## 4.10 Dissolution scallops

A particularly enigmatic pattern formation process during dissolution of rock (and melting of ice) under turbulent flow is the scalloping observed on cave walls (Fig. 4.14; Curl, 1966; Goodchild and Ford, 1971; Blumberg and Curl, 1974; Villien *et al*., 2005; Meakin and Jamtveit, 2010). Scallops have a characteristic size (wavelength) that depends inversely on flow velocity. As dissolution proceeds, the scallops migrate both normal to the wall, as the whole surface recedes, and in the direction of flow, while maintaining their shape and spacing. This shape stability requires a carefully controlled dissolution rate profile, that itself depends on the shape of the scallop and the resulting hydrodynamics. This self organisation of a stable but migrating pattern under such chaotic and unstable conditions is fascinating. While Bird *et al.* (2009) carried out 3D fluid dynamics simulation of flow over scallops, and Hammer *et al.* (2012) coupled a 2D turbulence model to a dissolution model and partly reproduced the dissolution profile required for shape stability (Fig. 4.15), the full natural pattern formation process has not yet been reproduced by computer simulation. This highlights the complexity and limited knowledge about reactive, turbulent flow coupled with dissolution or precipitation.

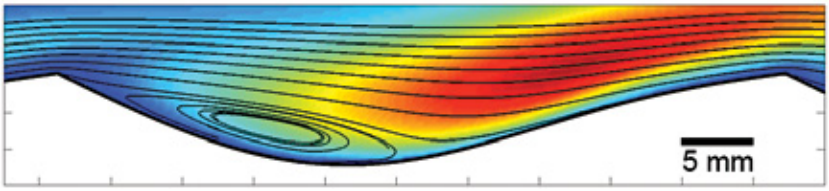


**Figure 4.15** Flow over dissolution scallops (from left to right) simulated by computational fluid dynamics techniques (k-ε turbulence modelling). The time averaged velocity field is shown as streamlines, while the eddy viscosity (turbulence) is indicated by the colour scale, where red is maximum and blue, minimum value. Flute wavelength is 5.1 cm (from Hammer *et al*., 2012, with permission from the National Speleological Society, www.caves.org).

## 4.11 Patterns controlled by air flow

Interactions between rocks and fluids can involve not only water but also air. A particularly interesting case is the phenomenon of *tafoni*, which are intricate weathering patterns formed by growth and coalescence of deep cavities on rock surfaces. Tafoni formation (at smaller scales known as honeycomb weathering, Fig. 4.16) has been studied extensively and it is generally believed that growth of salt crystals plays an important role (Bradley *et al*., 1978; McBride and Picard, 2004).

Huinink *et al*. (2004) presented an informative simulation of the growth of a single tafone cavity. They used a simple 2D model with a wet zone inside the rock, in which water flowed according to Darcy's equation for unsaturated flow (with a saturation dependent permeability and pressure) in a porous medium. Closer to the rock-air interface, there was a dry zone, where water vapour was modelled by the diffusion equation. The complex motion of water vapour in air inside the cavity was abstracted using a diffusion equation with a high diffusivity. The simulation was run in alternating steps of drying and wetting. Interestingly, the model indicated that in the regime of long drying periods, more salt is deposited inside the sheltered cavity, where the rate of drying is lower than outside. Consequently, salt weathering is enhanced inside the cavity. This mechanism provides the positive feedback loop necessary for localisation and growth of tafoni.

Photo: Bjørn Jamtveit.

**Figure 4.16** Honeycomb weathering of a gravestone, Whitby, England.

## 4.12 The role of biology

Microorganisms are present on most wet rock surfaces and many of us have had unfortunate experiences with the slippery biofilm that rapidly grows on immersed rocks. However, the role that microorganisms play in pattern formation is often uncertain. They can influence pattern formation but they do not necessarily change the nature of the pattern formation process and the mere presence of microorganisms does not imply that they exert a controlling influence over dissolution and/or precipitation. The interface between warm water and rocks provides a particularly favourable environment for microorganisms and they are abundant in the travertine hot springs illustrated in Figure 4.2. However, the strikingly large scale (one to tens of metre scale) travertine terraces shown in Figure 4.2 and the smaller scale morphologies can be explained without biological processes. Biofilm is also present during the formation of many cave speleothems and geyserite terraces and other patterns formed in wet environments. In all of these cases, it is common to find the mineralised remains of microorganisms entombed in the mineral deposits but it is also clear that the gross morphology can be explained by abiotic mechanisms alone. Consequently, the relative importance of biotic and abiotic processes remains undetermined and opinions vary greatly. In the case of travertine terraces, where growth is controlled by $CO_2$

degassing, the presence of a biofilm on the travertine water interface has little or no effect on the fluid dynamics, water chemistry or the transport of dissolved substances in the water.

In most biofilms, the diffusion coefficients of ions and small molecules are at least 10% of the diffusion coefficient in water and often substantially greater (Stewart, 2003). Therefore, biofilms have little effect on the transport of ions and small molecules to and from the rock surface unless the thickness of the biofilm is comparable with or larger than the thickness of the boundary layer and precipitation or dissolution is controlled by diffusion across the boundary layer. Consequently, microorganisms can be mere bystanders during pattern formation. Of course, microorganisms *can* play a critical role by secreting compounds that greatly increase or decrease the rate of precipitation or dissolution by adsorbing strongly on mineral surfaces. Organic material can provide surfaces on which minerals can nucleate and grow and by changing the composition of the fluid in the vicinity of the surface. However, biofilms might only exist on wet rock surfaces because the rock provides a foundation on which a biofilm can form and resist being washed away. In such a case, there might be no reason why the biofilm should have developed the ability to actively control dissolution and precipitation. The formation of patterns that have a striking resemblance to speleothems, travertine and geyserite terraces, scallops, etc. in ice strongly suggest that the formation of these patterns does not depend on biological processes.

## 4.13 A cold note on universality: bringing it all together

We have a fascination with general principles of pattern formation that are more or less independent of detailed mechanisms. Botryoidal growth in minerals and plants (Figs 3.4 and 4.6) is one example. This does not mean that we are uninterested in those mechanisms; on the contrary, identifying a general principle at work in a particular system can be an important tool for understanding the basic chemistry or physics. The idealised method, as illustrated by our travertine work, can be described as starting with a top down approach, first making hypotheses about overall systems properties, and then identifying processes. Finally, the procedure is reversed by simulating the detailed interactions in order to reconstruct the emergence of the pattern (the bottom up or reductionist phase).

A delightful example of such universality is the emergence of patterns in ice during melting or freezing (*cf.* Meakin and Jamtveit, 2010). These intricate patterns bear an uncanny resemblance to those forming during dissolution (melting) or precipitation (freezing) of limestone. We believe that the general pattern formation principles are the same, involving positive and negative feedbacks between dissolution, precipitation, transport and flow. Considering the detailed mechanisms, there is a curious analogy between the transport of $CO_2$ in the water phase in the case of carbonate rocks and the transport of heat in the case of ice. The mathematical equations for these two transport processes are more or less the same and similar patterns form as a result.

A few examples illustrate the case. *Ice terraces* (Streitz and Ettema, 2002) form in streams where water flows in a thin film or shallow depth and freezes on top of existing ice (so called *aufeis*). At small scales, such terraces look very similar to travertine microterraces. At larger scales, they form cascades that are almost indistinguishable from those in travertine (Fig. 4.17a). *Icicles* are stalactites, where ripples decorate the surface as for their limestone analogue (Fig. 4.17b and Ueno *et al.*, 2010). Spectacular dissolution scallops form on the walls of melt water tunnels in glaciers, just as in the analogous karst setting, and rillenkarst is a familiar sight on melting glaciers and ice cubes in drinks (Fig. 4.17c).

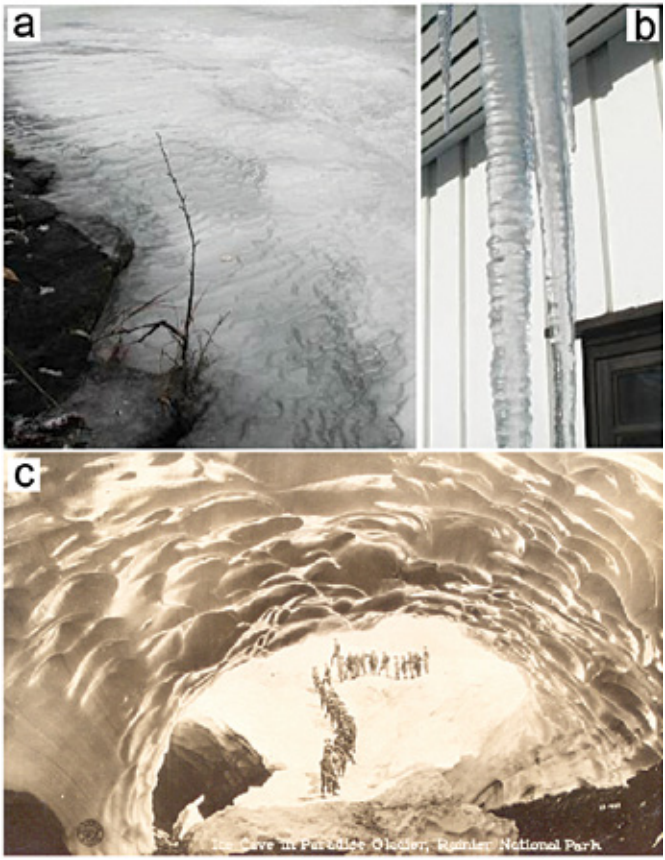


Photos: Øyvind Hammer.

**Figure 4.17** a) Ice terraces in a stream in Oslo. b) Rings on icicles. c) Photo from a vintage postcard showing scallops in the roof of the Paradise Glacier, Mount Rainier National Park. In 1978, this set of caves was the longest mapped system of glacier caves in the world but now the caves are completely gone because the glacier has receded.

# REFERENCES SECTION 4


BIRD, A.J., SPRINGER, G.S., BOSCH, R.F., CURL, R.L. (2009) Effects of surface morphologies on flow behaviour in karst conduits. *Proceedings, 15th International Congress of Speleology* 1417-1421.

BLUMBERG, P.N., CURL, R.L. (1974) Experimental and theoretical studies of dissolution roughness. *Journal of Fluid Mechanics* 65, 735-751.

BRADLEY, W.C, HUTTON, J.T., TWIDALE, C.R. (1978) Role of salts in development of granitic tafoni, South Australia. *Journal of Geology* 86, 647–654.

BUHMANN, D., DREYBRODT, W. (1985) The kinetics of calcite dissolution and precipitation in geologically relevant situations of karst areas. 1. Open system. *Chemical Geology* 48, 189-211.

CURL, R.L. (1966) Scallops and flutes. *Transactions of Cave Research Group* 7, 121-160.

GABROVŠEK, F. DREYBRODT, W. (2001) A model of the early evolution of karst aquifers in limestone in the dimensions of length and depth. *Journal of Hydrology* 240, 206-224.

GOLDENFELD, N., CHAN, P.-Y., VEYSEY, J. (2006) Dynamics of precipitation pattern formation at geothermal hot springs. *Physical Review Letters* 96, 254501.

GOODCHILD, M.F., FORD, D.C. (1971) Analysis of scallop patterns by simulation under controlled conditions. *Journal of Geology* 79, 52-62.

HAMMER, Ø. (1998) Regulation of astogeny in halysitid tabulates. *Acta Palaeontologica Polonica* 43, 635-651.

HAMMER, Ø. (2008) Pattern formation: Watch your step. *Nature Physics* 4, 265-266.

HAMMER, Ø., DYSTHE, D.K., JAMTVEIT, B. (2007) The dynamics of travertine dams. *Earth and Planetary Science Letters* 256, 258-263.

HAMMER, Ø., DYSTHE, D.K., LELU, B., LUND, H., MEAKIN, P., JAMTVEIT, B. (2008) Calcite precipitation instability under laminar, open-channel flow. *Geochimica et Cosmochimica Acta* 72, 5009-5021.

HAMMER, Ø., DYSTHE, D.K., JAMTVEIT, B. (2010) Travertine terracing: patterns and mechanisms. In: Pedley, H.M., Rogerson, M. (Eds) *Tufas and Speleothems: Unravelling the Microbial and Physical Controls*. Geological Society of London Special Publication 336, pp. 345-355.

HAMMER, Ø., LAURITZEN, S.E., JAMTVEIT, B. (2012) Stability of dissolution flutes under turbulent flow. *Journal of Cave and Karst Studies*, doi: 10.4311/2011JCKS0200 (in press).

HUININK, H.P., PEL, L., KOPINGA, K. (2004) Simulating the growth of tafoni. *Earth Surface Processes and Landforms* 29,1225-1233.

JETTESTUEN, E., JAMTVEIT, B., PODLADCHIKOV, Y.Y., DEVILLIERS, S., AMUNDSEN, H.E.F., MEAKIN, P. (2006) Growth and characterization of complex mineral surfaces. *Earth and Planetary Science Letters* 249, 108-118.

KAANDORP, J.A., KOOPMAN, E.A., SLOOT, P.M.A., BAK, R.P.M., VERMEIJ, M.J.A., LAMPMANN, L.E.H. (2003) Simulation and analysis of flow patterns around the scleractinian coral *Madracis mirabilis* (Duchassaing and Michelotti). *Philosophical Transactions of the Royal Society of London B* 358, 1551-1557.

KAANDORP, J.A., SLOOT, P.M.A., MERKS, R.M.H., BAK, R.P.M., VERMEIJ, M.J.A., MAIER, C. (2005) Morphogenesis of the branching coral *Madracis mirabilis*. *Proceedings of the Royal Society B* 272, 127-133.

MCBRIDE, E.F, PICARD, M.D. (2004) Origin of honeycombs and related weathering forms in Oligocene Macigno sandstone, Tuscan coast near Livorno, Italy. *Earth Surface Processes and Landforms* 29, 713–735.

MEAKIN, P. (1998) *Fractals, scaling and growth far from equilibrium*. Cambridge University Press.

MEAKIN, P., JAMTVEIT, B. (2010) Geological pattern formation by growth and dissolution in aqueous systems. *Proceedings of the Royal Society of London A* 466, 659-694.

MEAKIN, P., KRUG, J. (1990) Columnar microstructure in three-dimensional ballistic deposition. *Europhysics Letters* 11, 7-12.

SHORT, M.B., BAYGENTS, J.C., BECK, J.W., STONE, D.A., TOOMEY, R.S., GOLDSTEIN, R.E. (2005) Stalactite growth as a free-boundary problem: A geometric law and its Platonic ideal. *Physical Review Letters* 94, 018501.

STEWART, P.S. (2003) Diffusion in biofilms. *Journal of Bacteriology* 185, 1485-1491.

STREITZ, J.T., ETTEMA, R. (2002) Observations from an aufeis windtunnel. *Cold Regions Science and Technology* 34, 85-96.

UENO, K., FARZANEH, M., YAMAGUCHI, S., TSUJI, H. (2010). Numerical and experimental verification of a theoretical model of ripple formation in ice growth under supercooled water film flow. *Fluid Dynamics Research* 42, 025508.

VEYSEY, J., GOLDENFELD, N. (2008) Watching rocks grow. *Nature Physics* 4, 310-313.

VILLIEN, B., ZHENG, Y., LISTER, D. (2005) Surface dissolution and the development of scallops. *Chemical Engineering Communications* 192,125-136.